Mineralogical characterisation and separation studies on the recovery of Cr₂O₃ in the high carbon ferrochrome slag

Jing Chang [1], Hongjing Li [2], Kaidi Zheng [3], Chunguang Liu [2], Liming Wang [2], Biao Li [4], Xiangning Bu [3], Huaizhi Shao [3, 5]

[1] Department of Chemical and Materials Engineering, University of Alberta, Edmonton, T6G 1H9, Alberta, Canada

[2] Baogang Mining Research Institute, Baotou, 014010, Inner Mongolia, China

[3] Key Laboratory of Coal Processing and Efficient Utilization (Ministry of Education), School of Chemical Engineering and Technology, China University of Mining and Technology, Xuzhou 221116, Jiangsu, China

[4] Mining and Minerals Engineering Department, Virginia Tech, Blacksburg, Virginia 24060 US

[5] School of Resources and Environmental Engineering, Shandong University of Technology, Zibo 255049, China

Corresponding authors: shaohuaizhicumt@outlook.com (Huaizhi Shao), xiangning.bu@cumt.edu.cn (Xiangning Bu)

Abstract: In this study, the beneficiation performance of chrome from the high carbon ferrochrome slag (HCFS) was evaluated. The mineralogical characteristics of HCFS was investigated first, and then HCFS was treated by magnetic separation, gravity separation, magnetic-gravity combined separation, and gravity separation after grinding respectively, to recover the Cr₂O₃. Finally, the Fuerstenau upgrading curves were used to evaluate the separation performance of different separation processes. The results indicated that the gravity separation process with a proper grinding condition gave the optimum beneficiation performance. A concentrate product with 30.18% Cr₂O₃ grade and 22.52% recovery was obtained from the HCFS.

Keywords: high carbon ferrochrome slag, Cr₂O₃, physical separation, Fuerstenau upgrading curve

1. Introduction

Chromium (Cr) is a versatile element used in numerous applications in metallurgical, chemical, foundry sand, and refractory industries (Koleli and Demir, 2016). In the process of stainless steel smelting, a large amount of chromium was mainly lost in high carbon ferrochrome slag (HCFS) and fly ash (Daavittila et al., 2004; Jeremiah et al., 2006). Producing one megagram of high carbon ferrochrome can generate 1-3 megagram of HCFS (Bai et al., 2015). Huge amount of ferrochrome slag has been produced from submerged electric arc furnace during the manufacture of ferrochrome alloy. Furthermore, as a heavy metal, the residual chromium in the solid waste can endanger the environment (Bo et al., 2001; Dhal et al., 2013). This solid waste containing about 6-12% chromium as chromium oxide (highly immobile Cr(III) state) has the potential of transferring into highly leachable Cr(VI) state, which can lead to environment contamination (Panda et al., 2012).

Chromite (FeCr₂O₄) is a major commercially recoverable source of Cr, which accounts for nearly 90% of consumption. Chrome ores are mined globally, but South Africa holds approximately three-quarters of the world's viable chromite reserves. Conversely, the chromite in China are rare (0.15%) (Yang et al., 2018). Chrome ore in China are mostly met by imports (Pariser et al., 2018).

In view of the increase of the chromium slag and the serious environment problems, it is urgent and necessary to develop a comprehensive utilization of chromium slag. HCFS has been used in many applications, such as, concrete, road making and building materials, ceramic (Deakin et al., 2001; Sahu et al., 2016; Zhang et al., 2013). However, those processes have not completely recycled the chromium slag. HCFS is an important source of chromium metal (Mashanyare and Guest, 1997; Spooren et al., 2016; Van Staden et al., 2014; Xue et al., 2018). At present, the high-cost leaching method is the main

method to recycle the chromium in HCFS (Chen et al., 2014; Kim et al., 2016; Spooren et al., 2016). In addition, Bai et al. (Bai et al., 2015) investigated the effects of significant factors, namely the particle size, current, magnetic intensity and magnetic field intensity, on the magnetic separation performance for HCFS. They found that the optimal magnetic separation condition was achieved when the current reached 2.4 A and the particle size was above 150 μm, and the maximum percentage of chromium extracted from HCFS was 24.9%.

It is worthwhile to note that only few studies were focused on the separation of chrome from the HCFS using physical methods. In this study, the mineralogical characteristics of HCFS was investigated first, and then HCFS was treated by magnetic separation, gravity separation, and magnetic-gravity combined separation, respectively. Finally, the grade and recovery of chrome (Cr_2O_3 wt. %) of different processes were compared according to the Fuerstenau upgrading curves to explore the optimum separation condition.

2. Materials and methods

2.1. Materials

The HCFS sample was obtained from a ferrochrome plant of Mintal Group Co., Ltd in Inner Mongolia of China. The d_{80} of slag ranged from 3 to 5 mm, and the bulk density is 3.5 g/cm³. The chemical composition of the sample was measured by X-ray Fluorescence Spectrometer (XRF, S8 Tiger). The mineralogical phase was investigated by XRD analysis (Bruker D8 Advance, Germany) with a step size of 0.02° from 5 to 80° (2θ) using a D/MAX-2500 pc powder diffractometer equipped with Cu-Kα (λ= 1.54 Å) radiation generated at 40 mA and 40 kV. Table 1 shows the chemical composition of the samples. The Cr_2O_3 content of the sample was 8.92%. Fig. 1 shows the XRD results of the sample, and the mineralogical characterization indicated that the dominant mineral phases were forsterite, spinel, and mullite. The representative BSE images of the HCFS were provided in Fig. 2. Table 2 summarizes the Cr_2O_3 contents and respective assigned densities of the materials and phases identified. It was noted that the majority of chromium was present in the form of partial altered chromite (PAC), spinel, and entrapped alloy. Those materials with a high Cr_2O_3 content were regarded as valuable materials.

Table 1. Major chemical constituents from XRF analysis

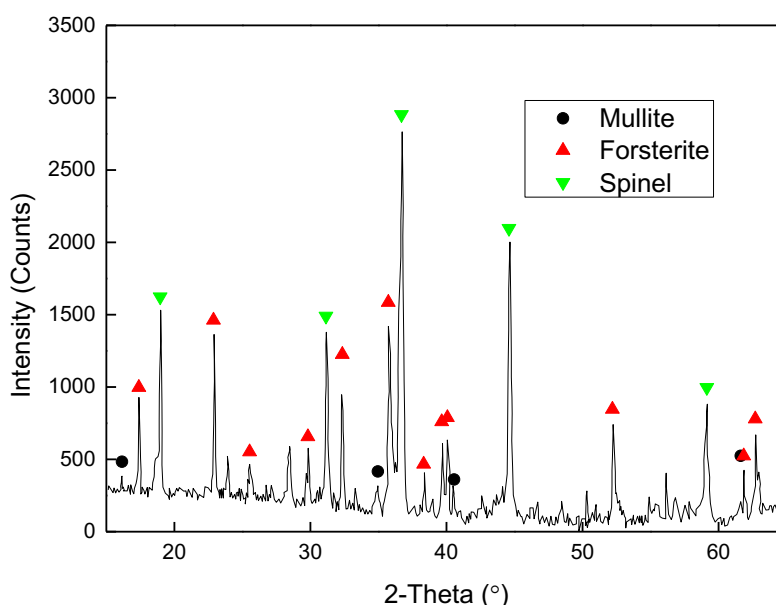| Chemical composition	Cr_2O_3	CaO	Al_2O_3	MgO	SiO_2	Fe_2O_3
Content (%)	8.92	3.3	30.6	21.8	28.24	4.40

Fig. 1. X-Ray Diffraction (XRD) study of the slag sample
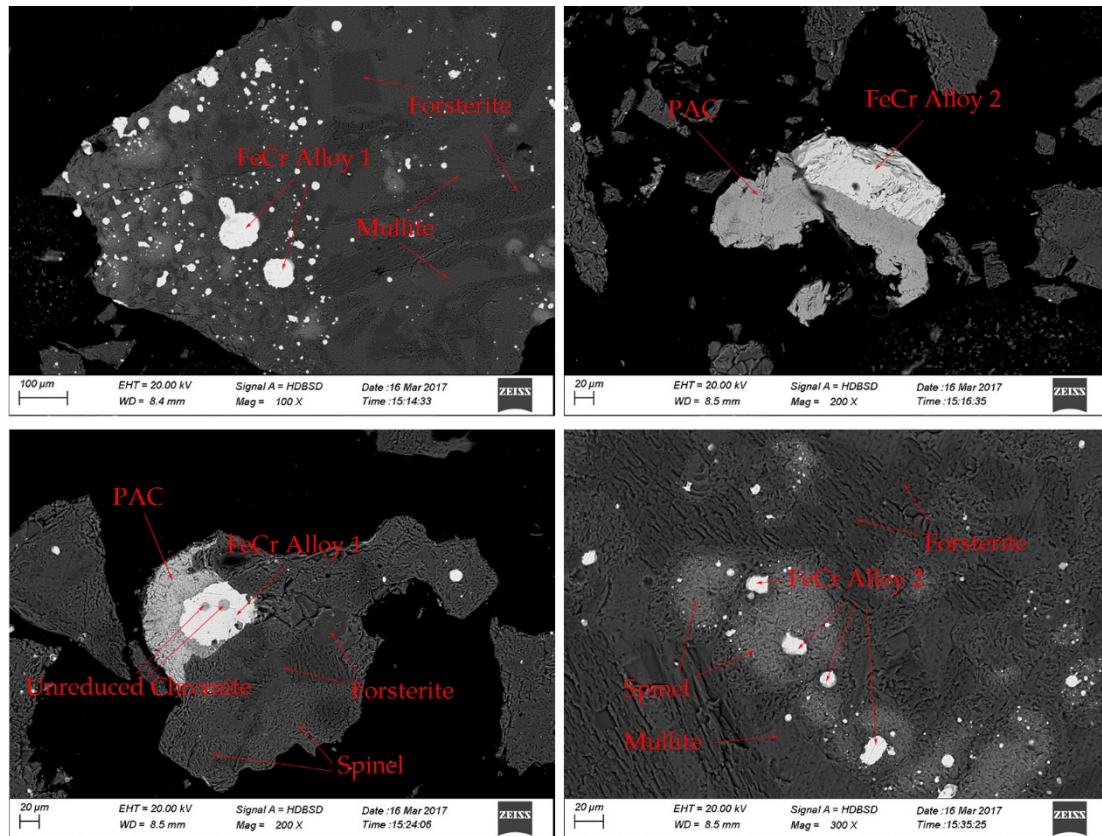
Fig. 2. The representative BSE images of the HCFS

Table 2. The Cr_2O_3 contents and respective assigned densities of the major materials and phases identified from XRF, XRD and SEM-EDS analysis

Material no.	Material name	Cr_2O_3	Assigned density (g/cm³) [a]
1	FeCr Alloy 1 (Carbide)	5.54	6.66
2	PAC	49.36	5.09
3	FeCr Alloy 2 (High Cr)	36.68	6.49
4	Spinel	22.59	4.06
5	Forsterite	3.59	3.35
6	Mullite	-	3.47

[a] Assigned density referred to the literature(Bergmann et al., 2016)

2.2. SEM-EDS

The polished thin-sections and sample blocks were coated with a thin layer of gold and imaged using a Zeiss scanning electron microscope (SEM) (model EVO-MA15) equipped with an Energy-dispersive X-ray (EDS) detector (Bruker, model X Flash 6130). SEM images were taken with a high definition back scatter detector (HDBSD) at 20.0 kV voltage and 40 mA beam current.

2.3 Grinding and separation tests

After being crushed to the maximum particle size under 2 mm, the slag samples (300 g) with 50% solid concentration were ground for 15, 20 and 25 mins, respectively, by a laboratory rod mill (RK/BM φ170×200, Wuhan Rock Crush Grand Equipment Manufacture Co., Ltd) and sieved with a 74 μm sieve by a laboratory screen machine.

The type of RK/CRS Φ400×300 and RK/CSQ 50×70 magnetic separators (Wuhan Rock Crush Grand Equipment Manufacture Co., Ltd) were used for different intensity wet magnetic separations at 15% solid concentration. XCY-37 1100×500 shaking table from Xichang Prospecting Machinery Factory was used for gravity separation in this study. Gravity separation tests were conducted at 20% of feed solid

concentration, 10 mm of shake amplitude, 5° of deck tilt angle, 5 dm³/min of wash water flow rate, and 400 cycles/min of shake frequency. The chemical composition of products obtained from grinding and separation tests was analyzed by XRF.

3. Results and discussion

3.1. Mineralogical analysis

The densities of the gangue materials like forsterite and mullite were smaller than 3.5 g/cm³. Meanwhile, the densities of the materials (PAC, FeCr Alloy 2, and spinel) with a high Cr_2O_3 content were greater than 4.0 g/cm³. Thus, chromium can be separated easily due to the significant density difference between them, while particle size should also be considered in the gravity separation process(Napier-Munn and Wills, 2005). In addition, magnetic separation is an effective method to recover the chromium present in the form of FeCr alloy from HCFS.

Particle size measurements from BSE images (about 100 images) were analyzed by the ImageJ software. The grain size of valuable materials (PAC, spinel, and entrapped alloy) was counted and their cumulative size distribution is given in Fig. 3. It was observed that most of valuable particles were distributed from 40 to 110 µm. Those valuable particles (d_{90}=110 µm, d_{50}=76 µm) were found to be associated with the gangue materials. Thus, it was necessary to grind and mill the HCFS to liberate valuable particles from the raw sample prior to the separation processes.
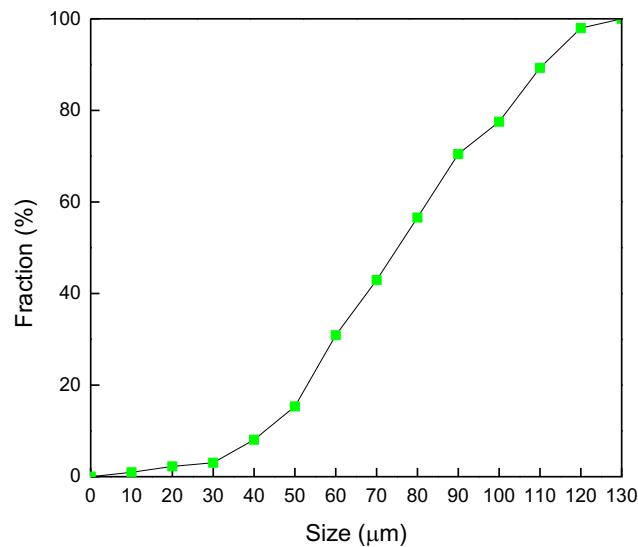

Fig 3. The cumulative size distribution of particles having a high Cr_2O_3 content in the HCFS

3.2. Analysis of grinding test

The results of the grinding tests are shown in Fig. 4. According to the Fig. 4, as the content of -74 µm fraction in the sample gradually increased, the grade of Cr_2O_3 was slightly improved. It indicates that the valuable and gangue minerals were both ground to below -74 µm. When the content of -74 µm fraction increased from 83.96% to 95.73%, the grade of Cr_2O_3 changed slightly, while the recovery of Cr_2O_3 increased. It indicated the liberation of chromium was greater with the increasing of the content of -74 µm fraction. The grade was changed probably because of the selective comminution between valuable materials and gangue materials. Similar reports can be found in the literature(Hesse et al., 2017; Tong et al., 2013).

3.3. Separation processes

3.3.1. Magnetic separation

The magnetic separation tests were conducted using two different samples, which have -74 µm particles contents of 83.96% and 95.73%, respectively, to determine the optimal separation intensity.
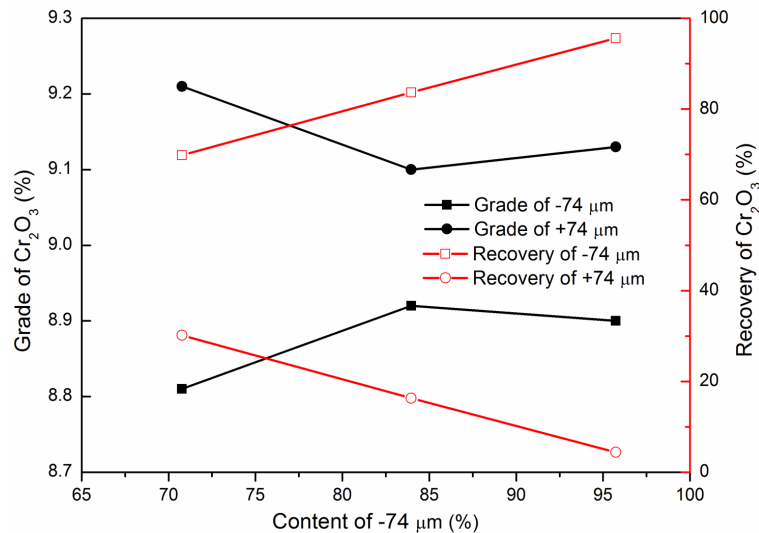
Fig. 4. Results of grinding tests

The low field intensity magnetic separation using 83.96% and 95.73% content of -74 μm fractions were performed, and the results are shown in Fig. 5. For 83.96% content of -74 μm fraction, with the increase of magnetic intensity, the recovery of Cr_2O_3 increased gradually, leading to a gradual decrease of the Cr_2O_3 grade. Comparing the results of the grade and the recovery of Cr_2O_3, the optimal separation field intensity was at 0.32 T, with the grade of Cr_2O_3 in the concentrate of 11.14% and the recovery of Cr_2O_3 of 54.78%. The similar trend of the grade and the recovery of Cr_2O_3 was also found for the separation using 95.73% content of -74 μm fraction.

The results manifested that the recovery of Cr_2O_3 increased gradually with the increase of magnetic field, which indicates that higher magnetic field is beneficial for the recovery of Cr_2O_3. When the content of -74 μm fraction increased from 83.96% to 95.73%, the recovery of Cr_2O_3 at 0.34 T magnetic intensity decreased from 54.13% to 29.78%, respectively, which means a large number of fine-grained valuable particles with weak magnetism were lost in the tailings of magnetic separation. Meanwhile, with the increase of the grinding fineness, the grade of Cr_2O_3 at 0.34 T increased from 11.22% to 12.80%. It implies that the increase of grinding fineness was also favorable to the liberation of valuable particles (rich resource of chromium) from the HCFS. When the fineness of grinding increased, the liberation of valuable materials was greater. Fine-grained weak magnetic FeCr alloy lost in the tailing would increase. Therefore, the grinding fineness should be selected based on the comprehensive evaluation of the recovery and the grade of Cr_2O_3.
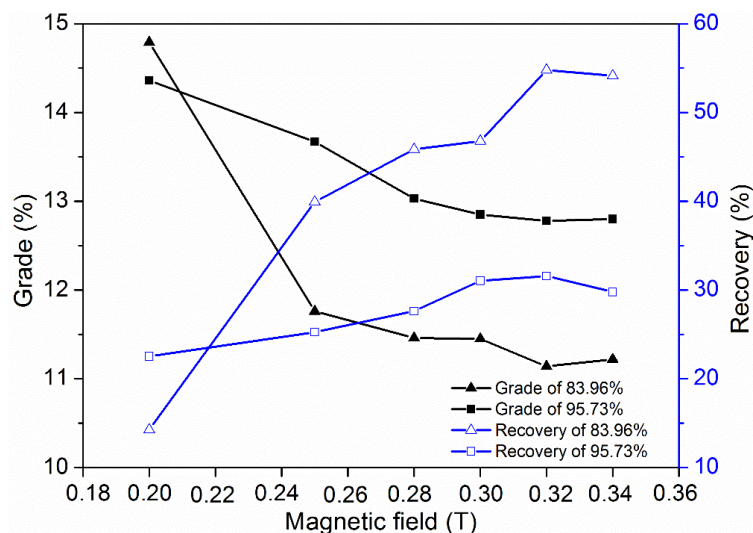

Fig. 5. Results of low intensity magnetic separation using 83.96% and 95.73% content of -74 μm fraction

The high intensity magnetic separation using 95.73% content of -74 µm fraction was studied in order to further explore the effect of magnetic field on the recovery of Cr_2O_3. The separation performance can be seen in Fig. 6. When the magnetic field increased from 0.6 to 2.0 T, the recovery of Cr_2O_3 increased gradually, while the grade of Cr_2O_3 decreased gradually. However, the magnetic field at 1.5 and 2.0 T was too high to be applied in practical work. Thus, the magnetic field at 1.0 T was the optimal high intensity magnetic separation. The Cr_2O_3 grade of 10.29% and the recovery of 76.01% were obtained, respectively.

From the above results of magnetic separation test, it can be found that the recovery of Cr_2O_3 increased with the increase of the magnetic field. However, the grade of Cr_2O_3 in the concentrate also decreased gradually. As the magnetic field increased, more and more liberated valuable particles and gangue particles were recovered, which led to an increase of the recovery of Cr_2O_3. Meanwhile, this also reduced the grade of Cr_2O_3 in the concentrate.
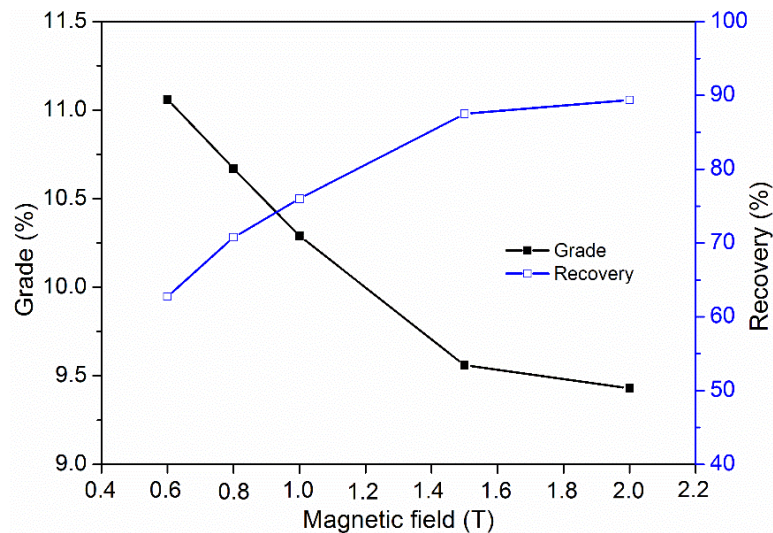

Fig. 6. Results of high intensity magnetic separation using 95.73% content of -74 µm fraction

3.3.2. Gravity separation

The gravity separation using 95.73% content of -74 µm fraction was performed with a shaking table. Fig. 7(a) shows the flow diagram of gravity separation. The results of gravity separation using shaking table were shown in Fig. 7(b). The grade and the recovery of Cr_2O_3 in the concentrate (C_1) were 30.17 % and 4.03 %, respectively. Moreover, the grade of Cr_2O_3 in the tailing (T_1) was still high (7.51 %) after two scavenging on the tailings. Under the microscope, the particle size distribution of valuable particles in the tailings were mainly around 20-50 µm, with a very small amount of about 100 µm particles. Thus, the performance of shaking table on the tailings was poor. This was mainly due to the liberation of small valuable particles (20-50 µm) in the tailings, which would be easily affected by the water flow. Those small particles cannot be separated according to the density difference and were lost in the tailings, thus resulting in a low recovery of Cr_2O_3.

3.3.3. Pre-grinding and gravity separation

In order to reduce the loss of valuable particles (20-50 µm) in the shaking table, the closed-circuit grinding setting was added to change the particle size of the feed before gravity separation. By avoiding the excessive grinding and increasing the average size of valuable particles, the screening size of 180 µm was used in the grinding process. Flow diagram of pre-grinding and gravity separation was illustrated in Fig. 8(a). The slag samples were pre-screened using the 1 mm and 180 µm screens. After being ground, the obtained particles (-180 µm) was separated by the shaking table.

Fig. 8(b) shows the results of pre-grinding and gravity separation. The grade and the recovery of Cr_2O_3 in the concentrate (C_1) was 30.18 % and 22.52 %, respectively. The separation efficiency was greatly improved, comparing to the gravity separation. The reason might be the shaking table could

recover a part of fine-grained valuable material, which were not over-grounded. It was worth mentioning that the shaking table still could not recover the fine particles with a particle size of 20-50 μm.

Overall, most of relatively valuable material larger than 50 μm were efficiently recover from the HCFS. Meanwhile, some parts of FeCr alloy in the tailings contain high amount of chromium and are wrapped with gangue slag, which cannot be separated by shaking table gravity separation due to their fine particle size (20-50 μm).
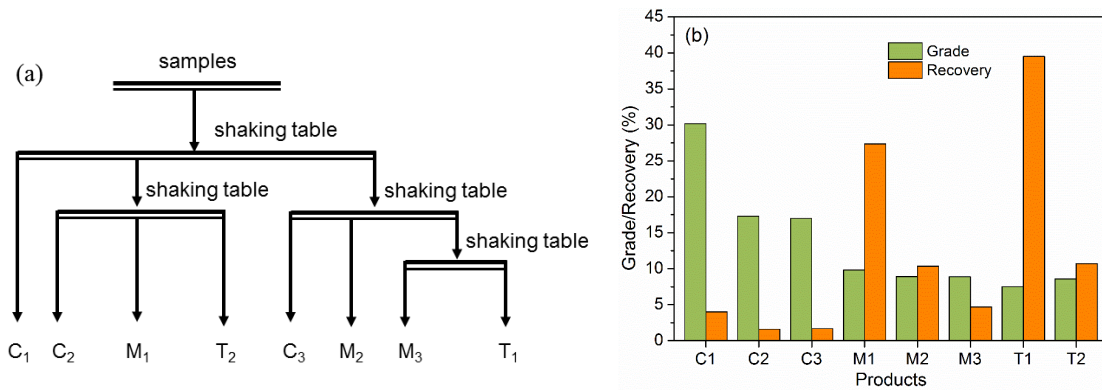

Fig. 7. Flow diagram (a) and the results (b) of gravity separation. C, M, and T represent concentrate, middling, and tailings, respectively
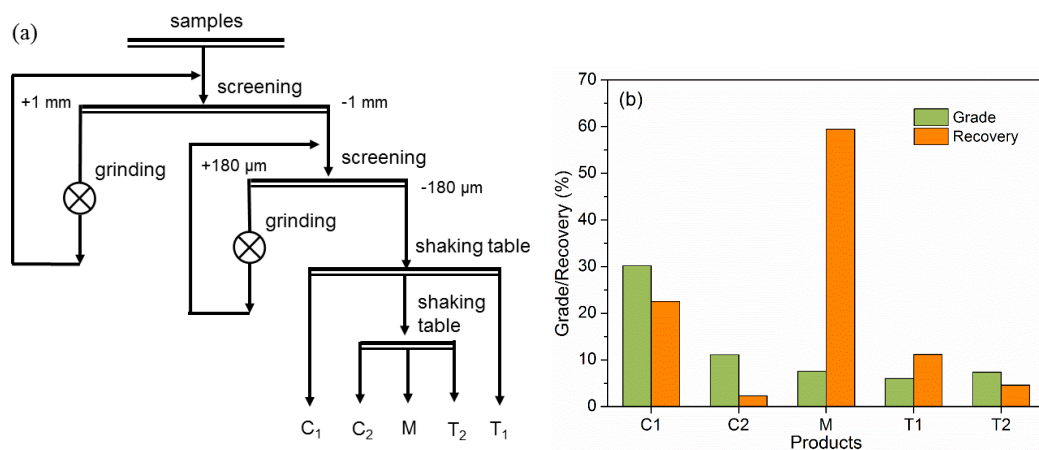

Fig. 8. Flow diagram (a) and the results (b) of pre-grinding and gravity separation. C, M, and T represent concentrate, middling, and tailings, respectively

3.3.4. Magnetic-gravity separation

The concentrate with higher grade can be obtained by the gravity separation, but the recovery was low. The higher recovery of Cr_2O_3 can be achieved by the magnetic separation, however the grade was still low because of the gangue minerals entrained in the concentrate. Therefore, the magnetic separation and gravity separation were combined to achieve higher recovery and higher grade of Cr_2O_3. Fig. 9(a) illustrates the flow diagram of magnetic-gravity separation. The magnetic separation was conducted using 95.73% content of -74 μm fraction at 1.0 T intensity, which was proved to be the optimal separation intensity. The gravity separation was carried out on the concentrate and the tailings obtained from the magnetic separation, respectively.

The results of magnetic-gravity separation are shown in Fig. 9(b). The grade and recovery of Cr_2O_3 in the concentrate were 31.60% and 5.49%, respectively. The grade and recovery of Cr_2O_3 in the combined tailings (T, M_1, M_2 and T_1) were 7.05 % and 61.37 %, respectively. The grade and recovery of Cr_2O_3 in the combined middling (M, C_1 and C_2) were 14.16 % and 33.14 %, respectively. To be noted,

the particle size of valuable particles in the middling was mainly of 20-50 µm, which could not be separated by shaking table more efficiently.
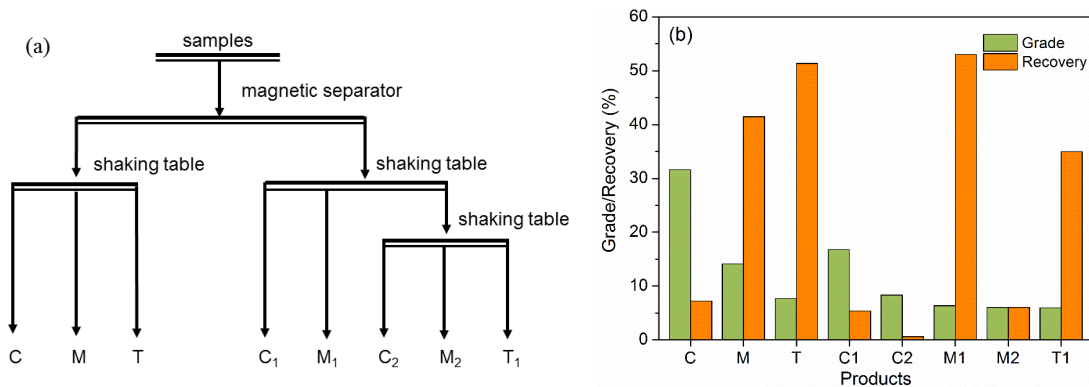

Fig. 9. Flow diagram (a) and the results (b) of magnetic-gravity separation. C, M, and T represent concentrate, middling, and tailings, respectively

3.4. Comparison of separation efficiency

The Fuerstenau upgrading curves have been widely used to compare and evaluate the separation efficiency in minerals processing, such as the separation of graphite (Bu et al., 2018), copper ore (Drzymala et al., 2013, 2010) and fine coals (Drzymala, 2005; Jia et al., 2002; Xing et al., 2017). According to Drzymala and Ahmed, there are many calculation equations for Fuerstenau upgrading curves, which could be used for the approximation of data (Drzymala and Ahmed, 2005). The equation used in this study containing only one adjustable parameter (α), which is given by:

$$R_C = \frac{100^\alpha - R_T^\alpha}{100^{\alpha-1}} \tag{1}$$

where, R_C and R_T stand for the recovery of valuable minerals in the concentrate and the gangue minerals in the tailing, respectively. a is the separation efficiency factor, which is used to assess the separation efficiency. When a is 0 or ∞, the separation is in ideal situation; when α is within 0 to 1, the upgrading process exists in the tailings; if α is equal to 1, there is no upgrading between valuable and gangue minerals; when $a>1$, then the upgrading process occurs in the concentrate. To be noted, the larger the value of α is, the better the separation efficiency is. In addition, the calculation equations of R_C and R_T are given below,

$$R_C = \frac{Y_C \times G_C}{G_{Total}} \tag{2}$$

$$R_T = \frac{Y_T \times (100 - G_T)}{100 - G_{Total}} \tag{3}$$

where, Y_C and G_C stand for the yield and grade of cumulative of concentrate, respectively. Y_T and G_T stand for the yield and grade of cumulative of tailings, respectively. G_{Total} stands for the total grade of Cr_2O_3.

The calculated results for the Fuerstenau upgrading curves of different separation processes is given in the Table 3. The Fuerstenau upgrading curves of different separation processes are shown in Fig. 10. The lines represent the Fuerstenau upgrading curves of different separation processes by fitting with their experimental results, represented by solid symbols. As can be seen from Fig. 10, the Fuerstenau upgrading curves agreed well with the experimental results.

Table 3 shows the separation efficiency factor (a) calculated by the Matlab software. When the adjusted coefficient of determination (R^2) was more than 0.80, it indicated that the model used had a good fit (Joglekar and May, 1987). Thus, the approximation of separation results could be calculated using Equation (1). a of pre-grinding and gravity separation was 4.281, which is much larger than other processes, indicating that the pre-grinding and gravity separation was the best process to recover the Cr_2O_3 in the slag. Compared to these experiments on -74 µm fraction, the gravity separation with -180 µm fraction achieved better separation performance in terms of recovery and grade. According to the

mineralogical analysis, the particle size of the majority of valuable materials ranged from 40 to 110 μm. With the grinding size of 74 μm, some valuable particles were over-ground to be smaller than 50 μm. Gravity separation is not an appropriate method for concentration for size classes finer than 50 μm. Thus, a reasonable grinding process can quickly recover the dissociated coarse-grained particles. This was probably the reason why the pre-grinding and gravity separation process had the highest efficiency among these processes. On the one hand, the overgrinding particles will reduce the recovery of chromium. On the other hand, they will lead to more entrainment of fine gangue particles, resulting in a decline of the Cr_2O_3 grade in the concentrate.
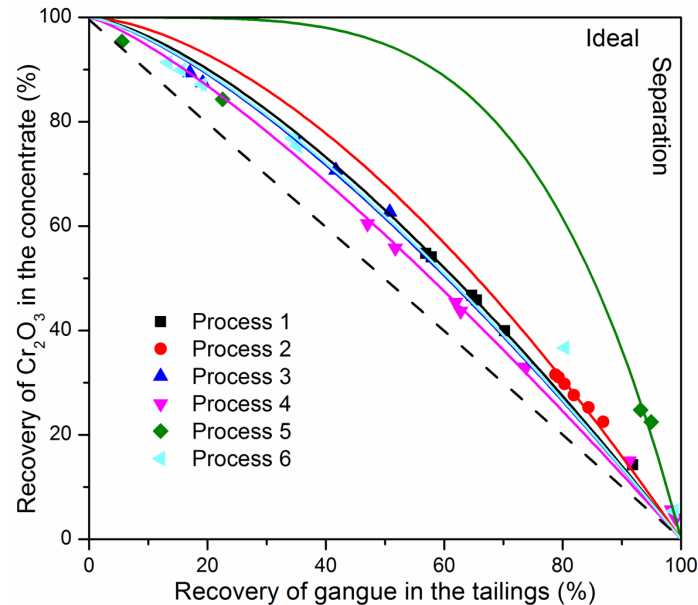

Fig. 10. Fuerstenau upgrading curves of different separation processes. Process 1-6 represent the low intensity magnetic separation on 83.96% and 95.73% content of -74 μm fraction; the high intensity magnetic separation on 95.73% content of -74 μm fraction; gravity separation on 95.73% content of -74 μm fraction; pre-grinding and gravity separation on -180 μm fraction; and magnetic-gravity separation on 95.73% content of -74 μm fraction, respectively. The dashed line represents for no separation

Table 3. Comparison of the efficiency factor and the optimum results of different separation processes

Separation processes	Model parameter		Concentrate	
	a	Adjusted R^2	Grade/%	Recovery/%
Process 1	1.438	0.9927	11.14	54.78
Process 2	1.641	0.9121	12.78	31.58
Process 3	1.379	0.9738	10.29	76.01
Process 4	1.263	0.9881	30.17	4.03
Process 5	4.281	0.9392	30.18	22.52
Process 6	1.393	0.9774	31.60	5.49

4. Conclusions

Mineralogical analysis indicated that the majority of chromium was present in the form of partial altered chromite (PAC), spinel, and entrapped alloy (regarded as valuable materials). The gangue materials were identified as forsterite and mullite. The average particle size (d_{50}) of those valuable materials was 76 μm, which was associated with the gangue materials. Compared to 180 μm grinding size, the liberation degree of valuable materials was higher with the grinding size of 74 μm, while an amount of valuable particles was over-ground and lost in the tailings. According to the differences of densities and permeability between valuable materials and gangue materials, gravity separation (shaking table) and magnetic separation (magnetic separators) techniques were employed to recover chromium from the

HCFS. Comparison of the Fuerstenau upgrading curves of various separation processes indicated that the pre-grinding and gravity separation process gave the highest separation efficiency, with 30.18% Cr_2O_3 grade and 22.52% recovery.

Acknowledgments

References

BAI, Z.T., ZHANG, Z.A., GUO, M., HOU, X.M., ZHANG, M., 2015. *Magnetic separation and extraction chrome from high carbon ferrochrome slag*. Mater. Res. Innov. 19, S2-113-S2-118.

BERGMANN, C., GOVENDER, V., CORFIELD, A.A., 2016. *Using mineralogical characterisation and process modelling to simulate the gravity recovery of ferrochrome fines*. Miner. Eng. 91, 2–15.

BO, B.L., FALLMAN, A.M., LARSSON, L.B., 2001. *Environmental impact of ferrochrome slag in road construction*. Waste Manag. 21, 255–264.

BU, X., ZHANG, T., CHEN, Y., PENG, Y., XIE, G., WU, E., 2018. *Comparison of mechanical flotation cell and cyclonic microbubble flotation column in terms of separation performance for fine graphite*. Physicochem. Probl. Miner. Process.

CHEN, G., WANG, X., DU, H., ZHANG, YING, WANG, J., ZHENG, S., ZHANG, YI, 2014. *A clean and efficient leaching process for chromite ore*. Miner. Eng. 60, 60–68.

DAAVITTILA, J., HONKANIEMI, M., JOKINEN, P., 2004. *The transformation of ferrochromium smelting technologies during the last decades*. J. South African Inst. Min. Metall. 104.

DEAKIN, D., WEST, L.J., STEWART, D.I., YARDLEY, B.W.D., 2001. *Leaching behaviour of a chromium smelter waste heap*. Waste Manag. 21, 265–270.

DHAL, B., THATOI, H.N., DAS, N.N., PANDEY, B.D., 2013. *Chemical and microbial remediation of hexavalent chromium from contaminated soil and mining/metallurgical solid waste: A review*. J. Hazard. Mater. 250–251, 272–291.

DRZYMALA, J., 2005. *Evaluation and comparison of separation performance for varying feed composition and scattered separation results*. Int. J. Miner. Process. 75, 189–196.

DRZYMALA, J., AHMEND, H.A.M., 2005. *Mathematical equations for approximation of separation results using the Fuerstenau upgrading curves*. Int. J. Miner. Process. 76, 55–65.

DRZYMALA, J., KOWALCZUK, P.B., OTENG-PEPRAH, M., FOSZCZ, D., MUSZER, A., HENC, T., LUSZCZKIEWICZ, A., 2013. *Application of the grade-recovery curve in the batch flotation of Polish copper ore ✭*. Miner. Eng. 49, 17–23.

DRZYMALA, J., LUSZCZKIEWICZ, A., FOSZCZ, D., 2010. *Application of Upgrading Curves for Evaluation of Past, Present, and Future Performance of a Separation Plant*. Miner. Process. Extr. Metall. Rev. 31, 165–175.

HESSE, M., POPOV, O., LIEDERWIRTH, H., 2017. *Increasing efficiency by selective comminution*. Miner. Eng. 103, 112–126.

JEREMIAH, J., LAURA, S., GRAEDEL, T.E., 2006. *The contemporary anthropogenic chromium cycle*. Environ. Sci. Technol. 40, 7060–7069.

JIA, R., HARRIS, G.H., FUERSTENAU, D.W., 2002. *Chemical Reagents for Enhanced Coal Flotation*. Coal Prep. 22, 123–149.

JOGLEKAR, A.M., MAY, A.T., 1987. *Product excellence through design of experiments*. Cereal foods world 32, 857.

KIM, E., SPOOREN, J., BROOS, K., NIELSEN, P., HORCKMANS, L., VRANCKEN, K.C., QUAGHEBEUR, M., 2016. *New method for selective Cr recovery from stainless steel slag by NaOCl assisted alkaline leaching and consecutive BaCrO 4 precipitation*. Chem. Eng. J. 295, 542–551.

KOLELI, N., DEMIR, A., 2016. *Chromite*, in: Prasad, M.N. V, Shih, K.B.T.-E.M. and W. (Eds.), Environmental Materials and Waste: Resource Recovery and Pollution Prevention. Academic Press, pp. 245–263.

MASHANYARE, H.P., GUEST, R.N., 1997. *The recovery of ferrochrome from slag at Zimasco*. Miner. Eng. 10, 1253–1258.

NAPIER-MUNN, T., WILLS, B.A., 2005. *Wills' Mineral Processing Technology*. Wills' Miner. Process. Technol. https://doi.org/10.1016/B978-0-7506-4450-1.X5000-0

PANDA, C.R., MISHRA, K.K., NAYAK, B.D., RAO, D.S., NAYAK, B.B., 2012. *Release behaviour of chromium from ferrochrome slag*. Int. J. Environ. Technol. Manag. 15, 261–274.

PARISER, H.H., BACKEBERG, N.R., MASSON, O.C.M., BEDDER, J.C.M., 2018. *Changing nickel and chromium stainless steel markets - a review*. J. South. African Inst. Min. Metall.

SAHU, N., BISWAS, A., KAPURE, G.U., 2016. *A Short Review on Utilization of Ferrochromium Slag*. Miner. Process. Extr. Metall. Rev. 37, 211–219.

SPOOREN, J., KIM, E., HORCKMANS, L., BROOS, K., NIELSEN, P., QUAGHEBEUR, M., 2016. *In-situ chromium and vanadium recovery of landfilled ferrochromium and stainless steel slags*. Chem. Eng. J. 303, 359–368.

TONG, L., KLEIN, B., ZANIN, M., QUAST, K., SKINNER, W., ADDAI-MENSAH, J., ROBINSON, D., 2013. *Stirred milling kinetics of siliceous goethitic nickel laterite for selective comminution*. Miner. Eng. 49, 109–115.

VAN STADEN, Y., BEUKES, J.P., VAN ZYL, P.G., DU TOIT, J.S., DAWSON, N.F., 2014. *Characterisation and liberation of chromium from fine ferrochrome waste materials*. Miner. Eng. 56, 112–120.

XING, Y., GUI, X., CAO, Y., WANG, Y., XU, M., WANG, D., LI, C., 2017. *Effect of compound collector and blending frother on froth stability and flotation performance of oxidized coal*. Powder Technol. 305, 166–173.

XUE, K., HAN, J., JIAO, F., LIU, W., QIN, W., CAI, L., XU, T., 2018. *Comprehensive utilization of spent magnesia-chrome refractories with gravity separation followed by flotation*. Miner. Eng. 127, 125–133.

YANG, Y., ZENG, L., DENG, F., HU, J., 2018. *Geological characteristics and mineralization potential of chromite resources in China*. Earth Sci. Front. 25, 138-147 (in Chinese).

ZHANG, T., PENG, G., GAO, P., WEI, J., YU, Q., 2013. *Effectiveness of novel and traditional methods to incorporate industrial wastes in cementitious materials – An overview*. Resour. Conserv. Recycl. 74, 134–143.